Hindawi
Mathematical Problems in Engineering
Volume 2018, Article ID 5325034, 14 pages
https://doi.org/10.1155/2018/5325034

Research Article

Self-Assisted First-Fix Method for A-BDS Receivers with Medium- and Long-Term Ephemeris Extension

Zilong Shen,[1,2] **Jing Peng**,[1] **Wenxiang Liu**,[1] **Feixue Wang**,[1] **Shibing Zhu**,[2] **and Zhongwang Wu**[2]

[1]*College of Electronic Science, National University of Defense Technology, Changsha 410073, China*
[2]*College of Space Information, Space Engineering University, Beijing 101416, China*

Correspondence should be addressed to Jing Peng; pengjing@nudt.edu.cn

Received 17 March 2018; Revised 20 May 2018; Accepted 12 June 2018; Published 25 July 2018

Academic Editor: Antonio Elipe

As a sensor for standalone position and velocity determination, the BeiDou Navigation Satellite System (BDS) receiver is becoming an important part of the intelligent logistics systems under rapid development in China. The applications in the mass market urgently require the BDS receivers to improve the performance of such functions, that is, shorter Time to First Fix (TTFF) and faster navigation signal acquisition speed with Ephemeris Extension (EE) in standalone mode. As a practical way to improve such functions of the Assisted BDS (A-BDS) receivers without the need for specialized hardware support, a Self-Assisted First-Fix (SAFF) method with medium- and long-term EE is proposed in this paper. In this SAFF method, the dynamic Medium- and Long-Term Orbit Prediction (MLTOP) method, which uses the historical broadcast ephemeris data with the optimal configuration of the dynamic models and orbit fitting time interval, is utilized to generate the extended ephemeris. To demonstrate the performance of the MLTOP method used in the SAFF method, a suit of tests, which were based on the real data of broadcast ephemeris and precise ephemeris, were carried out. In terms of the positioning accuracy, the overall performance of the SAFF method is illustrated. Based on the characteristics of the medium- and long-term EE, the simulation tests for the SAFF method were conducted. Results show that, for the SAFF method with medium- and long-term EE of the BeiDou MEO/IGSO satellites, the horizontal positioning accuracy is about 12 meters, and the overall positioning accuracy is about 25 meters. The results also indicate that, for the BeiDou satellites with different orbit types, the optimal configurations of the MLTOP method are different.

1. Introduction

At present, the BeiDou Navigation Satellite System (BDS), as one of the four major Global Navigation Satellite Systems (GNSSs)[1], has been providing reliable Positioning, Navigation, and Timing (PNT) services in Asia and Pacific areas [2, 3]. The BDS receivers, in the applications of intelligent logistics, intelligent Unmanned Aerial Vehicles (UAV), and Location-Based Services (LBS), can be seen as the important sensors for position and velocity determination [1, 4]. By the year of 2017, Over 90% of context-aware apps rely on GNSS service [1]. In the process of advancing applications of BDS receivers to the mass market, it is of great value to reduce the Time to First Fix (TTFF) and increase the navigation signal acquisition speed of the BDS receivers with Ephemeris Extension (EE) in standalone mode [5, 6]. Mass market LBS applications require high availability, a fast Time to First Fix (TTFF), and moderate accuracy [7]. Simultaneously, they need to preserve the battery life of the device and keep the cost of the GNSS receiver down [1]. The available ephemeris information plays an important role in these features of the self-assisted GNSS receivers. As a practical way to improve the usability of satellite ephemeris, the historical broadcast ephemeris data, already stored in the receiver, can be used to predict the Medium- and Long-Term Orbit (MLTO) and satellite clock data of the BeiDou satellites [8, 9]. Above all, the BDS receiver, to achieve the shortest TTFF [9], should adopt the Self-Assisted First Fix (SAFF) methods with the medium- and long-term extended ephemeris.

In recent years, several research studies have been carried out on the topic of First-Fix method of the assisted GNSS receivers. In the challenging environment, [10] studied the

First-Fix method with the long-term EE for GPS receivers. The User Range Error (URE) index is used to evaluate the accuracy of the extended ephemeris in four weeks and the accuracy of the First-Fix method with long-term EE. By contrast, the BDS system has mixed constellation of satellites. Consequently, for the BDS receiver, it is necessary to analyze the First-Fix method with medium- and long-term EE. Based on the characteristics of the satellites in the mixed constellation, studies should focus on the application model of the extended ephemeris in the SAFF method, and the performance should be evaluated. For the multi-GNSS receivers, [11] evaluated the accuracy and availability of the First-Fix method with long-term EE. The use of multi-GNSS satellites can improve the accuracy and availability of the First-Fix method. However, a detailed study of the MLTOP method for the BeiDou satellites was not carried out. The formula of the URE index is not suited to the BeiDou GEO/IGSO satellites. For the MLTOP method, [12] studied the use of ground observation data for predicting the high-precision long-term ephemeris of the GPS satellites. Additionally, this method is based on the satellite dynamic model. However, this method, for collecting enough observation data, requires the use of ground reference stations with accurately known coordinates. As a consequence, the timeliness of this method is poor and the amount of computation is large. However, the long-term ephemeris data with more precision can be predicted by this method. Reference [13] devised a long-term Ephemeris Extension method for GNSS satellites and indicated that, with extending ephemeris of good quality, the TTFF of the GNSS receivers can be reduced to 5~15s.

The Ephemeris Extension method has been implemented in some practical applications in the industry and can be used to obtain high-precision predicted ephemeris from different organizations. Rx Networks offers commercialized extended ephemeris services. This service can work in dual mode [14]. In the network connection mode, the extended ephemeris data service can be acquired through the network connection. Taking into account the high-speed transmission rate and lower cost of the mobile communication service provided by current cellular network, when the mobile device is in the network connection mode, it can get better extended ephemeris service performance. For example, JPL conducts the precise orbit determination of the navigation satellite constellation through a global tracking network and generates high-precision long-term predicted orbits. The URE of the predicted orbit data after 7 days is better than 10 meters. The extended ephemeris data released by JPL can be published via FTP service [15]. When the mobile device is in roaming mode, it can autonomously generate the extended ephemeris for the next 5 days [14].

For the BeiDou satellites of different orbit types, the optimal configurations of the Ephemeris Extension method should be different. In addition, with the long-term EE of satellites in the mixed constellation, the performance of the SAFF method should also be evaluated. This problem requires further in-depth research. The paper concerns the development of an efficient SAFF method with medium- and long-term EE for the BDS receivers, which needs necessary amount of historical broadcast ephemeris data as small as possible, without sacrificing the results accuracy too much. We also aim to provide more data records about the SAFF method with medium- and long-term EE of the BeiDou satellites, which can provide some guidelines for the design of advanced Assisted BDS (A-BDS) receivers.

This paper is organized as follows. Section 2 compares the First Fix of the conventional BDS receiver with the First Fix of the A-BDS receiver, provides theoretical description of the MLTOP methods, and analyzes the influence of EE on the First Fix. Section 3 presents the error statistics and time-consumption of the MLTOP method for the BeiDou MEO/IGSO satellites, compares the results with different orbit fitting time interval length, and then performs the accuracy assessment of the SAFF method with medium- and long-term EE. Finally, Section 4 draws the conclusions.

2. Self-Assisted First-Fix Method with Ephemeris Extension

2.1. Assisting the First Fix with Ephemeris Extension. Depending on the a priori information in the BDS receiver, the start mode of the BDS receiver can be divided into the following: cold start mode, warm start mode, and hot start mode [16]. The typical startup process of the conventional BDS receiver, with no assistance information, is shown in Figure 1. The startup process consists of signal acquisition and tracking, bit synchronization, frame synchronization, navigation message decoding, and position estimation. For the conventional BDS receiver with no assistance information, the time-consumption of the correlation lock and phase lock is approximately 1~2s. After that, the time-consumption of the bit synchronization and frame synchronization is approximately 6~12s. When the BDS receiver completes the frame synchronization process, the time of transmission has been already decoded from the second-of-week (SOW) data at the head of the BDS navigation message, and the full pseudorange measurement can be obtained. The receiving and decoding process of the complete ephemeris takes at least 30s. When the ephemeris data and pseudorange measurement for the sufficient number of BeiDou satellites have already been obtained, the First Fix can be performed immediately. So the TTFF of the conventional BDS receiver is at least 37s.

For the A-BDS receiver with EE, the navigation message decoding process can be skipped. When the EE process is performed by the receiver itself in standalone mode using the historical broadcast ephemeris, the receiver is in self-assisted mode. The significant advantage of the self-assisted BDS receiver is that, without the need for any communication connection, it can always be in standalone mode.

To reduce the TTFF of the BDS receiver, the EE can provide available ephemeris information. When the BDS receiver is in hot start mode, it is not necessary to perform the process of EE at all. However, if the process of EE has already been performed by the BDS receiver in cold start mode or warm start mode, the TTFF can be reduced about 20s, since there is no need for decoding the navigation message to obtain the real-time broadcast ephemeris. In addition, for the signal acquisition process of the BDS receiver in cold

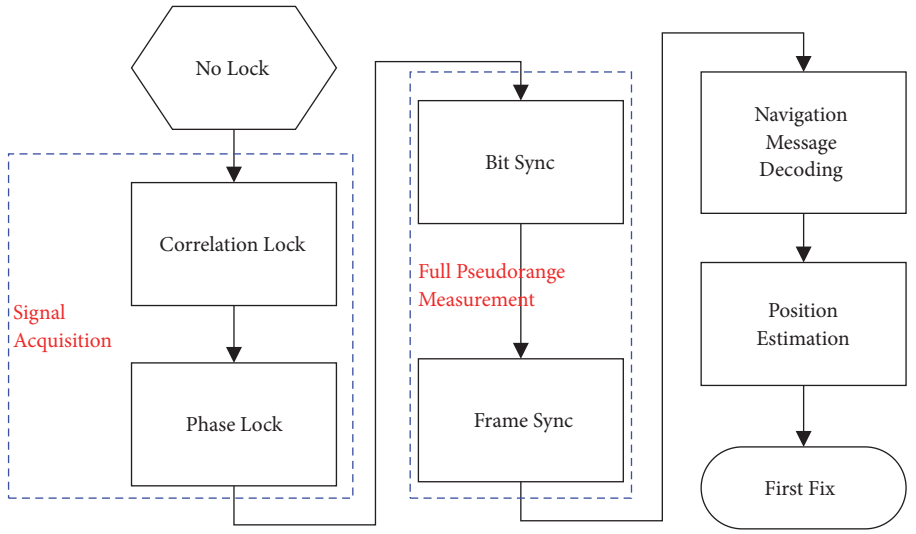

Figure 1: The typical startup process of the conventional BDS receiver with no assist information.

start mode or warm start mode, the extended ephemeris data can be used to reduce the search space of code-delay and frequency, and the corresponding time-consumption is reduced at the same time.

Due to the large amount of energy that needs to be consumed in the acquisition phase of the navigation signal, satellite navigation signal acquisition can be accelerated by using the autonomously extended ephemeris, thereby saving limited battery resources of the mobile device. The performance requirements of the hardware signal acquisition circuit for the acquisition phase can also be reduced.

2.2. Medium- and Long-Term Ephemeris Extension. The forces acting on the BeiDou satellites include the central gravity and the disturbing forces. The main disturbing forces are the noncentral attracting force of the Earth, the N-body gravity caused by the Sun and the Moon, the Solar Radiation Pressure (SRP) effect, the Earth solid tides, ocean tides, and the relativistic effect. The motion equations of the satellite described by the dynamic model are shown as follows [17]:

$$\ddot{\mathbf{r}} = -\mu\frac{\mathbf{r}}{r^3} + \mathbf{a}\left(t, \mathbf{r}, \dot{\mathbf{r}}, p_1, p_2, \ldots\right) = \mathbf{f}\left(t, \mathbf{r}, \dot{\mathbf{r}}, \mathbf{p}\right), \tag{1}$$

where μ is gravitational constant of the Earth, $\mathbf{r}$ is the position vector of the satellite in the Earth Centered Inertial (ECI) coordinate system, r is the distance from the satellite to the origin of the ECI coordinate system, $-\mu(\mathbf{r}/r^3)$ is the acceleration of central gravity, $\mathbf{a}$ is the perturbation acceleration of the satellite motion, $\mathbf{f}$ is the total acceleration of the satellite motion, and $\mathbf{p} = p_1, p_2, \ldots$ are the parameters of the disturbing force models.

The state vector of the navigation satellite is $\mathbf{y}(t) = \begin{pmatrix}\mathbf{r}\\ \dot{\mathbf{r}}\end{pmatrix}$. Simultaneously perform first-order differentials on both sides of the above equation, and the result is as follows:

$$\frac{d}{dt}\mathbf{y}(t) = \tilde{\mathbf{f}}\left(\mathbf{y}, t\right) = \begin{pmatrix}\dot{\mathbf{r}}\\ \mathbf{f}\end{pmatrix}. \tag{2}$$

Both sides of (2) are simultaneously doing partial differentials with respect to $\mathbf{y}(t_0)$, and the result is as follows:

$$\begin{aligned}\frac{\partial}{\partial \mathbf{y}\left(t_0\right)}\frac{d}{dt}\mathbf{y}(t) &= \frac{\partial \tilde{\mathbf{f}}}{\partial \mathbf{y}\left(t_0\right)} = \frac{\partial \tilde{\mathbf{f}}}{\partial \mathbf{y}(t)}\cdot\frac{\partial \mathbf{y}(t)}{\partial \mathbf{y}\left(t_0\right)}\\ &= \frac{d}{dt}\left(\frac{\partial \mathbf{y}(t)}{\partial \mathbf{y}\left(t_0\right)}\right).\end{aligned} \tag{3}$$

If we use the state transition matrix $\mathbf{\Phi}$, (4) can be obtained.

$$\frac{d}{dt}\mathbf{\Phi} = \frac{\partial \tilde{\mathbf{f}}\left(\mathbf{y}, t\right)}{\partial \mathbf{y}(t)}\cdot\mathbf{\Phi}, \tag{4}$$

$$\mathbf{\Phi} = \frac{\partial \mathbf{y}(t)}{\partial \mathbf{y}\left(t_0\right)} \tag{5}$$

$$\frac{\partial \tilde{\mathbf{f}}\left(\mathbf{y}, t\right)}{\partial \mathbf{y}(t)} = \begin{pmatrix}\mathbf{0}_{3x3} & \mathbf{I}_{3x3}\\ \dfrac{\partial \mathbf{f}}{\partial \mathbf{r}} & \dfrac{\partial \mathbf{f}}{\partial \dot{\mathbf{r}}}\end{pmatrix}_{6x6} \tag{6}$$

Following the processing method of the equations above, (7) can be obtained.

$$\frac{d}{dt}\frac{\partial \mathbf{y}(t)}{\partial \mathbf{p}} = \frac{\partial \tilde{\mathbf{f}}\left(\mathbf{y}, t, \mathbf{p}\right)}{\partial \mathbf{y}(t)}\cdot\frac{\partial \mathbf{y}(t)}{\partial \mathbf{p}} + \frac{\partial \tilde{\mathbf{f}}\left(\mathbf{y}, t, \mathbf{p}\right)}{\partial \mathbf{p}}, \tag{7}$$

$$\mathbf{S} = \frac{\partial \mathbf{y}(t)}{\partial \mathbf{p}} \tag{8}$$

$$\frac{d}{dt}\mathbf{S} = \begin{pmatrix}\mathbf{0}_{3\times3} & \mathbf{I}_{3\times3}\\ \dfrac{\partial \mathbf{f}}{\partial \mathbf{r}} & \dfrac{\partial \mathbf{f}}{\partial \dot{\mathbf{r}}}\end{pmatrix}_{6\times6}\cdot\mathbf{S} + \begin{pmatrix}\mathbf{0}_{3\times n_p}\\ \dfrac{\partial \mathbf{f}}{\partial \mathbf{p}}\end{pmatrix}_{6\times n_p} \tag{9}$$

The set of differential equations can be transformed to the following equations [17, 18]:

$$\frac{d}{dt}(\boldsymbol{\Phi}\ \ \mathbf{S}) = \begin{pmatrix} \mathbf{0}_{3\times3} & \mathbf{I}_{3\times3} \\ \dfrac{\partial \mathbf{f}}{\partial \mathbf{r}} & \dfrac{\partial \mathbf{f}}{\partial \dot{\mathbf{r}}} \end{pmatrix}_{6\times6} (\boldsymbol{\Phi}\ \ \mathbf{S}) + \begin{pmatrix} \mathbf{0}_{3\times6} & \mathbf{0}_{3\times n_p} \\ \mathbf{0}_{3\times6} & \dfrac{\partial \mathbf{f}}{\partial \mathbf{p}} \end{pmatrix}_{6\times(6+n_p)}, \tag{10}$$

$$\boldsymbol{\Phi}(t_0) = \mathbf{I}, \tag{11}$$

$$\mathbf{S}(t_0) = \mathbf{0}, \tag{12}$$

$$\widetilde{\boldsymbol{\Phi}} = \begin{pmatrix} \boldsymbol{\Phi} & \mathbf{S} \\ \mathbf{0}_{n_p\times6} & \mathbf{I}_{n_p\times n_p} \end{pmatrix} = \begin{pmatrix} \dfrac{\partial \mathbf{r}}{\partial \mathbf{r}_0} & \dfrac{\partial \mathbf{r}}{\partial \dot{\mathbf{r}}_0} & \dfrac{\partial \mathbf{r}}{\partial \mathbf{p}} \\ \dfrac{\partial \dot{\mathbf{r}}}{\partial \mathbf{r}_0} & \dfrac{\partial \dot{\mathbf{r}}}{\partial \dot{\mathbf{r}}_0} & \dfrac{\partial \dot{\mathbf{r}}}{\partial \mathbf{p}} \\ \mathbf{0}_{n_p\times3} & \mathbf{0}_{n_p\times3} & \mathbf{I}_{n_p\times n_p} \end{pmatrix}, \tag{13}$$

$$\mathbf{A} = \begin{pmatrix} \mathbf{0}_{3\times3} & \mathbf{1}_{3\times3} & \mathbf{0}_{3\times n_p} \\ \dfrac{\partial \mathbf{a}}{\partial \mathbf{r}} & \dfrac{\partial \mathbf{a}}{\partial \mathbf{v}} & \dfrac{\partial \mathbf{a}}{\partial \mathbf{p}} \\ \mathbf{0}_{n_p\times3} & \mathbf{0}_{n_p\times3} & \mathbf{0}_{n_p\times n_p} \end{pmatrix}_{(6+n_p)\times(6+n_p)}. \tag{14}$$

Then (10) can be transformed into (15).

$$\frac{d}{dt}\widetilde{\boldsymbol{\Phi}} = A\widetilde{\boldsymbol{\Phi}}, \tag{15}$$

Together with the satellite state vector related differential equations, we can form the following first-order differential equations:

$$\frac{d}{dt}\begin{pmatrix} \mathbf{r} \\ \dot{\mathbf{r}} \\ \widetilde{\boldsymbol{\Phi}} \end{pmatrix} = \mathbf{A}\begin{pmatrix} \dot{\mathbf{r}} \\ \mathbf{f} \\ \widetilde{\boldsymbol{\Phi}} \end{pmatrix}. \tag{16}$$

The initial conditions for first-order differential equation are described by (17).

$$\widetilde{\boldsymbol{\Phi}}(t_0) = \begin{pmatrix} \mathbf{I}_{6\times6} & \mathbf{0}_{6\times n_p} \\ \mathbf{0}_{n_p\times6} & \mathbf{I}_{n_p\times n_p} \end{pmatrix}, \quad \begin{pmatrix} \mathbf{r} \\ \dot{\mathbf{r}} \end{pmatrix}_{t_0} = \begin{pmatrix} \mathbf{r}(t_0) \\ \dot{\mathbf{r}}(t_0) \end{pmatrix} \tag{17}$$

where $\boldsymbol{\Phi}$ is the state transition matrix, $\mathbf{S}$ is the sensitivity matrix that includes the partial derivatives of the satellite's state parameters with respect to the force model parameter vector, n_p is the length of the force model parameter vector, t_0 is the initial epoch, $\mathbf{r}_0$ is the position of the satellite at the initial epoch, $\dot{\mathbf{r}}_0$ is the velocity of the satellite at initial epoch, and $\mathbf{p}$ is the force model parameter vector.

To solve the set of differential equations described by (16) and (17), the numerical integration method can be used. Commonly used numerical integration methods are the Runge-Kutta method, the Adams-Bashforth-Moulton method, the Adams-Cowell method, and so on [17]. For the scenarios of the MLTOP, the 7th-order Runge-Kutta-Fehlberg integrator RKF7(8) can be used in the orbit integration process [19].

The position data of the satellite, which are obtained by using the historical broadcast ephemeris stored in the receiver, are used as the virtual observations [20]. At epoch t, the observation equation of the satellite is shown as follows:

$$y_t = h\left(\overrightarrow{X}\right) + \varepsilon, \tag{18}$$

where $\overrightarrow{X}$ is the state vector of the satellite at epoch t, ε is the measurement error, and y_t is the virtual observation at epoch t. The Least Squares (LS) fitting method can be used to solve the observation equations to obtain the state vector of the satellite and the force model parameter vector at the initial epoch.

Supposing that the state transition matrix at epoch t is Φ_t, the sensitivity matrix at epoch t is S_t, and t_0 is the initial epoch, the residual vector V can be given by

$$V = y_t - h\left(\overrightarrow{X}(t_0)\right) = H \cdot (\Phi_t\ \ S_t) \cdot \Delta q + \varepsilon', \tag{19}$$

$$H = \frac{\partial h\left(\overrightarrow{X}(t_0)\right)}{\partial \overrightarrow{X}(t_0)}, \tag{20}$$

$$\Delta q = (\Delta r_0\ \ \Delta \dot{r}_0\ \ \Delta p), \tag{21}$$

where H is the Jacobian that gives the partial derivatives of the modeled observations with respect to the state vector and the force model parameters of the satellite at the initial epoch t_0, h is a function of the state vector and the force model parameters of the satellite at the initial epoch t_0, and Δq is the error of the initial value of r_0, $\dot{r}_0$, and p. Δq can be obtained by the LS fitting method.

The satellite's initial state vector is estimated through orbit fitting process using the historical broadcast ephemeris data, and the improvement of the orbit initial vector is performed by the orbit fitting algorithm. The initial value of the satellite's initial state vector can be obtained using the historical broadcast ephemeris or using the ultrarapid precise ephemeris products generated by IGS networks [21], which is determined by the conditions of the assistance information of mobile devices. However, the basic method is to use historical broadcast ephemeris data.

When the mobile device generates the extended ephemeris in autonomous mode, it is necessary to take into account the coordinate transformation between the inertial system and the ECEF coordinate system. At this time, it is necessary to estimate the earth orientation parameter, which includes polar motion parameters and time difference parameter. The EOP parameters can be estimated as elements

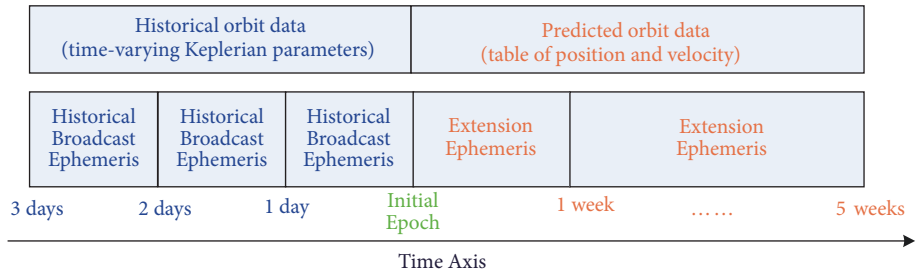

Figure 2: The data I/O of the dynamic MLTOP method for A-BDS receivers.

of the initial vector of the orbit fitting process. Together with the satellite's position, velocity, and the solar radiation pressure parameters of the initial epoch [22], it can be improved in the orbit fitting process. In other words, the initial vector to be estimated is first given an initial value, and then the observations obtained from the historical broadcast ephemeris data can be used to improve the initial vector.

Considering that, for the A-GNSS receiver, the network data service can be obtained through the mobile communication module, the IERS agency provides the rapid service and prediction product bulletin A weekly update file, through which the polar motion parameters and UT1-UTC value of the next year can be predicted, updated every Thursday. For the MEO satellites whose orbit characteristics are similar to those of GPS satellites, the orbit prediction errors caused by the predicted EOP parameters for one day are roughly distributed at 0.232 ± 0.183 m, and the orbit prediction errors caused by the predicted EOP parameters for 7 days are roughly distributed at 0.438 ± 0.356 m [23]. The EOP prediction data can be used during orbit fitting and orbit prediction. In particular, the standard EOP parameter data can be obtained from the IERS during the orbit fitting process [24]. The quality of the standard data is higher than that of the predicted products; thus, better prediction accuracy can be obtained.

In the networked state, assistance information may be obtained from 3G/4G communication link, including the precise ephemeris data, the predicted EOP parameters, historical broadcast ephemeris data, and ultrarapid precise ephemeris. Given the huge user capacity of future 5G mobile network [25], better data sharing technologies, and rapid and economical data transmission rate [25], it is also feasible to obtain one-week predicted EOP parameters or perform on-demand coordinate conversions of the predicted orbit data based on standard EOP data. When the A-BDS receiver is in a nonnetworked state or roams from an area within cellular network coverage to an area beyond the cellular network coverage, the predicted EOP parameters already received can support the Ephemeris Extension for the coming week without causing a large performance degradation of the First Fix. Based on standardized data sharing services, it can provide a solid foundation for future intelligent transformation of A-GNSS technology and service.

When there is a data service through network communication, the method used in this paper can use the latest mobile communication technology to obtain historical broadcasting ephemeris data from other cooperative or collaborative smartphone users. In the future 5G communication technologies, digital cellular networks will rely more on GNSS technology for time synchronization [1]. Common cellular network base stations will be equipped with high-precision GNSS modules. In the networked state, auxiliary broadcast ephemeris may be obtained from 5G communication base stations, even the precise ephemeris data and the predicted EOP parameters, historical broadcast ephemeris data, and ultrarapid precision ephemeris [21] for the autonomous Ephemeris Extension.

For nonnetworked terminal devices, pluggable memory cards or the Bluetooth technology can be used to transfer basic assistance data set, such as one-week predicted EOP data, historical broadcast ephemeris data, or ultrarapid precision ephemeris data [21] from computers or other networked devices. When it is used completely independently on a device without network connection, it is necessary to predict the EOP parameters or to estimate the EOP parameters together with the satellite initial state vector under certain optimal criteria [22].

The data Input and Output (I/O) of the dynamic MLTOP method are illustrated in Figure 2, where the initial epoch is the epoch of the orbit fitting solution, which is also the start point of orbit integration for EE. The format of the predicted orbit data is table of position and velocity, which is different from that of the historical orbit data. To get the position and velocity of the satellites at any epoch, we can use the interpolation method with the predicted orbit data.

The process of the dynamic MLTOP method consists of two main components, that is, the orbit fitting process and the orbit prediction process. The test process of the dynamic MLTOP method is depicted in Figure 3. Before the start of the orbit fitting process, the related parameters are set. During the operation of the test program, the time-consumption values of the orbit fitting process and the orbit prediction process are recorded. After the end of the orbit prediction process, the error statistics of the orbit prediction results are calculated.

For the medium- and long-term EE of BeiDou satellites, the MLTO accuracy of the BeiDou GEO satellites is too low to be used in the First Fix, and when using the extended ephemeris, the orbit data and clock data of the same navigation satellite must be used together. Therefore, we no longer study the medium- and long-term clock bias prediction of the BeiDou GEO satellites. Taking the BeiDou Pseudo Random Noise (PRN) 04 GEO satellite as an example,

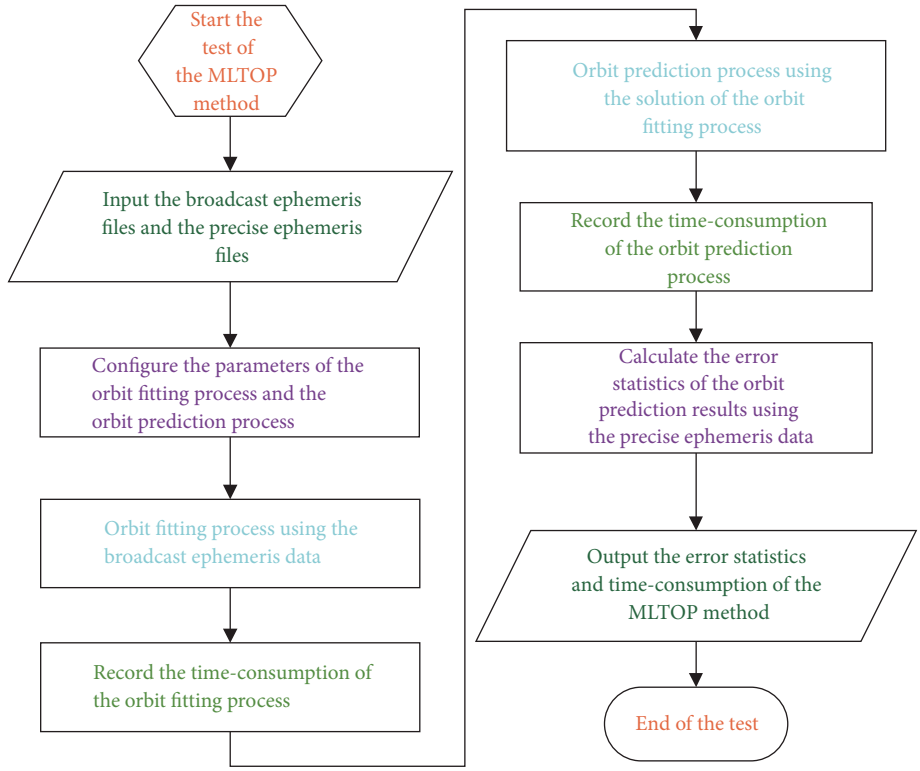

Figure 3: The test process of the dynamic MLTOP method for the BeiDou satellites.

for orbit prediction in the first week with the 30∗30-order EGM-96 model, the radial error is about 41 km.

To assess the accuracy of the BeiDou MEO/IGSO satellites clock bias prediction, we chose to use the broadcast ephemeris data and the precise satellite clock data within two periods of time, from 2016-09-10 to 2016-09-18 and from 2017-02-04 to 2017-02-14, respectively. The precise satellite clock data were obtained from the IGMAS project, the corresponding data interval is 5 minutes, and the broadcast ephemeris data, which were obtained from the IGS-MGEX project, were used for the parameter fitting of the satellite clock bias prediction model.

For the clock bias prediction of the PRN 10 BeiDou IGSO satellite, the prediction time length was 7 days, the broadcast ephemeris data of 2 days were used in the process of satellite clock bias prediction model parameter fitting, and the fitting step was 5 minutes. Compared with the precise clock data, the errors of the medium- and long-term satellite clock bias prediction for the BeiDou PRN 10 satellite were obtained in two tests, which were conducted and set at different time periods. In Test 1, the dates of the broadcast ephemeris data were 2016-09-08 to 2016-09-11, and the dates of the precision ephemeris data were 2016-09-08 to 2016-09-18. In Test 2, the dates of the broadcast ephemeris data were 2017-02-04 to 2017-02-07, and the dates of the precision ephemeris data were 2017-02-04 to 2017-02-14. The errors of prediction results are shown in Figure 4.

In Figure 4, the first 2 days of data are used for the fitting of the satellite clock bias model. From Figure 4, it can be seen that the maximum value of the prediction results error in Test 1 is about 17 meters, that is, about 56 nanoseconds, while in Test 2, the maximum value of the prediction results error is about 20 meters, that is, about 66 nanoseconds.

2.3. Position Estimation with Ephemeris Extension of BeiDou MEO/IGSO Satellites. To maintain its correct position in the Earth's geosynchronous orbit, the frequent orbit maneuver of the BeiDou GEO satellite was introduced [26], which greatly degraded the precision level of the MLTOP method that used the historical broadcast ephemeris data. For the BeiDou GEO satellites, the dynamic MLTOP method described above is not as effective as that of the BeiDou MEO/IGSO satellites. However, the GEO satellites are always visible in most areas of China, and the transmission rate of the GEO satellites' broadcast ephemeris is 10 times that of the MEO/IGSO satellites; the BDS receivers can quickly obtain the complete set of the GEO satellites' broadcast ephemeris data [27]. Currently, our theoretical and experimental works are focused on the EE of the BeiDou MEO/IGSO satellites.

The process of completing the frame synchronization needs to extract the second-of-week data segment located in the head of the navigation message subframe and usually takes 1 to 2 subframes to complete the second-of-week data segment extraction of all visible navigation satellites, thus completing the frame synchronization process. For BeiDou navigation satellites, each subframe header of the D1 type navigation message and D2 type navigation message transmits the second-of-week data segment; the transmission time of

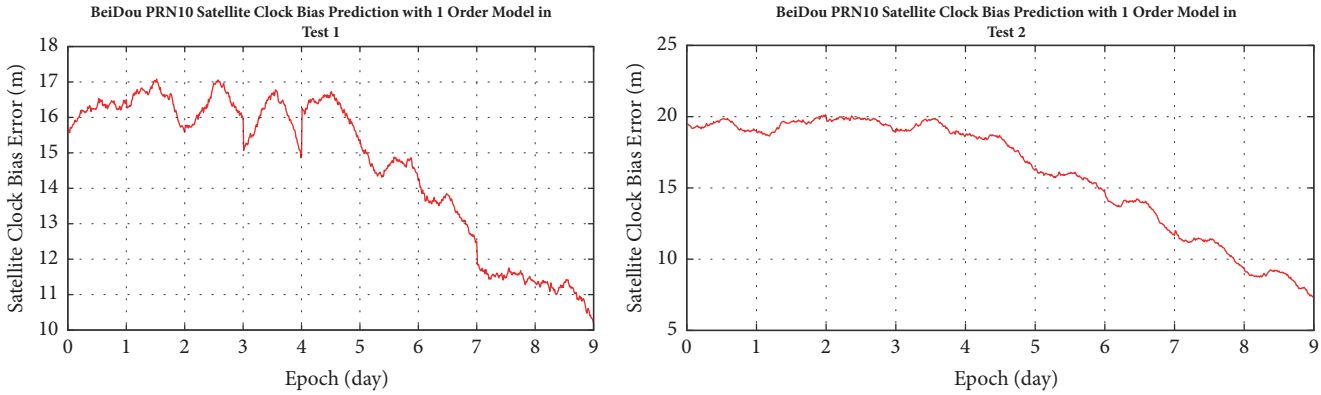

Figure 4: The error of satellite clock bias prediction results for BeiDou PRN 10 satellite in Test 1 and Test 2.

each D1 type navigation message subframe is 6 seconds and the transmission time of each D2 type navigation message subframe is 0.6 seconds [27]. For BeiDou MEO/IGSO satellites, the corresponding navigation message type is D1, and the time-consumption for completing the reception of 1 to 2 subframes is about 6 to 12 seconds.

For the BDS receiver, if there is no assistance information of approximate position, the receiver can use the BeiDou GEO satellites to complete the task of coarse positioning [27]; since the transmission rate of the GEO satellites is about 10 times that of the IGSO/MEO satellites, it costs 6~12s to complete the frame synchronization of the BeiDou MEO/IGSO satellites, during which the receiver can quickly complete the process of frame synchronization and navigation message decoding for all the BeiDou GEO satellites. So the corresponding TTFF is about 8~14 seconds, which is very close to the related results provided in [13].

3. Results and Discussion

Based on real broadcast ephemeris data and precise ephemeris products, tests were carried out to evaluate the performance of the SAFF method and the dynamic MLTOP method used in it. The broadcast ephemeris data are obtained from the International GNSS Service Multi-GNSS Experiment (IGS-MGEX) project [28], and the precise ephemeris products are obtained from the International GNSS Monitoring & Assessment System (IGMAS) project [29].

The experimental data of this paper are as follows: use the precision ephemeris data as the reference satellite ephemeris data, and use the broadcast ephemeris data as the historical ephemeris data. In order to support the study in this paper, two experiments were conducted and set at different time periods. In Test 1, the dates of the broadcast ephemeris data were 2016-09-08 to 2016-09-11. The dates of the precision ephemeris data were 2016-09-08 to 2016-09-18. In Test 2, the dates of the broadcast ephemeris data were 2017-02-04 to 2017-02-07. The dates of the precision ephemeris data were 2017-02-04 to 2017-02-14. By selecting data from different time periods for testing, we can verify the compatibility and consistency of the dynamic MLTOP method proposed in this paper. Compared with the orbit data obtained from the precise ephemeris file, the accuracy statistics of the MLTO data are calculated. In the designed tests of SAFF method, the maximum time length of the prediction orbit arc was set to be 1 weeks. As for the orbit fitting process, the fitting time interval was 3 days at maximum.

The computer environment of the SAFF prototype program is as follows: the operating system was 64bit Microsoft WIN7 SP1, the processor was Intel (R) Pentium (R) CPU G645 @ 2.90 GHz, and the programming environment consisted of 64bit Matlab R2017a and Microsoft Visual studio 2012. The orbit integration module of the prototype program was programmed in the C/C++ language, which could simulate the actual program in the BDS receivers, since the actual program in the embedded platform was usually programmed in the C language, while the observation simulation module, the data I/O module, and the results evaluation module were programmed in the Matlab language, which is convenient for the configuration parameters adjustment and the results logging and plotting.

To analyze different configurations of the fitting time interval length and their influence on the accuracy and time-consumption of the dynamic MLTOP method, different sets of experiments were designed, respectively. For the BeiDou MEO satellite, the time interval length of the satellite orbit fitting is set to 2 hours, 6 hours, 12 hours, 18 hours, and 24 hours, respectively. For the BeiDou IGSO satellites, the time interval length for satellite orbit fitting is set to 6 hours, 12 hours, 18 hours, 24 hours, 30 hours, 36 hours, and 42 hours, respectively. The effect of orbit fitting time interval length on the accuracy and time-consumption of MLTOP method is evaluated by the above experiments.

When using the historical broadcast ephemeris, the time interval between the contiguous fitting points is 15 minutes. Once the initial state vector and the force parameter vector are obtained from the LS fitting method, the orbit integration method is used to predict the MLTO data, of which the time interval between the contiguous prediction points is 15 minutes.

For the MLTO data in the Earth Centered Earth Fixed (ECEF) coordinate system, the errors in the X, Y, and Z axis directions, the errors in the radial, along-track, cross-track

(RAC) directions, and the 3D RMS error are calculated, respectively. The URE without considering the effect of satellite clock bias error is calculated as follows [30]:

$$URE = \sqrt{(0.980R)^2 + (0.141A)^2 + (0.141C)^2}, \quad (22)$$

where R is the error of the orbit data in the radial direction, A is the error of the orbit data in the along-track direction, and C is the error of the orbit data in the cross-track direction. From (22), it can be seen that the URE is mainly affected by the satellite orbit data error in the radial direction. So, in the tests, the MLTOP results errors in the radial direction were chosen as an important evaluation index.

Suppose that the user is on the surface of the earth and the cutoff angle is 0 degrees; the radius of the Earth is 6371 kilometers. The height of the BeiDou MEO satellite orbit is 21,528 kilometers. The height of the GEO/IGSO satellite orbit is 35,786 kilometers. The correlation coefficient between the satellite clock error and the orbital radial error is ρ_{rT}. Suppose that R is the error of the orbit data in the radial direction, A is the error of the orbit data in the along-track direction, C is the error of the orbit data in the cross-track direction, and T is the satellite clock bias error.

When $\rho_{rT} = -1$, the URE calculation formula for BeiDou MEO/GEO/IGSO satellites is as follows:

$$URE_{BDS} = \begin{cases} \sqrt{(0.99R - T)^2 + \frac{1}{127}\left(A^2 + C^2\right)} & MEO \\ \sqrt{(0.98R - T)^2 + \frac{1}{54}\left(A^2 + C^2\right)} & \frac{GEO}{IGSO}. \end{cases} \quad (23)$$

When $\rho_{rT} = 0$, the URE calculation formula for BeiDou MEO/GEO/IGSO satellites is as follows:

$$URE_{BDS} = \begin{cases} \sqrt{(0.99R)^2 + \frac{1}{127}\left(A^2 + C^2\right) + T^2} & MEO \\ \sqrt{(0.98R)^2 + \frac{1}{54}\left(A^2 + C^2\right) + T^2} & \frac{GEO}{IGSO}. \end{cases} \quad (24)$$

When $\rho_{rT} = 1$, the URE calculation formula for BeiDou MEO/GEO/IGSO satellites is as follows:

$$URE_{BDS} = \begin{cases} \sqrt{(0.99R + T)^2 + \frac{1}{127}\left(A^2 + C^2\right)} & MEO \\ \sqrt{(0.98R + T)^2 + \frac{1}{54}\left(A^2 + C^2\right)} & \frac{GEO}{IGSO}. \end{cases} \quad (25)$$

The value of ρ_{rT} is determined by the specific conditions. For the GPS system, $\rho_{rT} = -1$ [31].

In order to assess the accuracy of the SAFF method with long-term EE, we used two evaluation indexes, that is, the Circular Error Probable (CEP) and Spherical Error Probable (SEP), which are used to evaluate the horizontal positioning accuracy and overall positioning accuracy, respectively. The CEP and SEP are calculated as follows [32]:

$$CEP = \begin{cases} 0.562\sigma_E + 0.615\sigma_N & \sigma_E \geq \sigma_N \\ 0.615\sigma_E + 0.562\sigma_N & \sigma_E < \sigma_N, \end{cases} \quad (26)$$

$$SEP = \overline{\sigma} \cdot \left(1 - \frac{d}{9}\right)^{3/2}, \quad (27)$$

$$\overline{\sigma}^2 = {\sigma_E}^2 + {\sigma_N}^2 + {\sigma_U}^2, \quad (28)$$

$$d = \frac{2\left({\sigma_E}^4 + {\sigma_N}^4 + {\sigma_U}^4\right)}{\overline{\sigma}^4}, \quad (29)$$

where σ_E, σ_N, and σ_U are the error RMS value in the East, North, and Up axis directions of the ENU coordinate system.

3.1. The Tests of the Ephemeris Extension with Different Configurations. In order to reduce the time-consumption of the dynamic MLTOP method, we need to optimize the time interval length of the BeiDou satellites orbit fitting. In the configuration of the dynamic MLTOP method in the designed tests, use the 10∗10-order EGM-96 model, consider the influence of the N-body gravity produced by the Sun and the Moon, consider the effect of the SRP, and neglect the effects of the Earth solid tides, the pole tides, and the relativistic effect. In order to save space and facilitate comparative analysis, only the statistical results of the 3D error and the radial error are given.

For the BeiDou MEO satellite in all the tests, the length of the fitting time interval was chosen as 2 hours, 6 hours, 12 hours, 18 hours, and 24 hours in turn. The corresponding results of the 3D error are shown in Table 1, the corresponding results of the radial error are shown in Table 2 and Figure 5, and the corresponding time-consumption of the fitting process for PRN 11 satellite in Test 1 was 2.43s, 2.10s, 3.13s, 5.57s, and 6.80s, respectively. Since the difference of the time interval length for orbit fitting does not affect the time length of the orbit prediction process, the time interval length of the orbit prediction process is no longer analyzed here. For the BeiDou IGSO satellite in the tests, the length of the orbit fitting interval was chosen as 6 hours, 12 hours, 18 hours, 24 hours, 30 hours, 36 hours, and 42 hours in turn. The corresponding results of the 3D error are shown in Table 3, the corresponding results of the radial error are shown in Table 4 and Figure 6, and the corresponding time-consumption of the fitting process for PRN 6 satellite in Test 1 was 3.20s, 2.91s, 8.08s, 11.1s, 5.57s, 25.9s, and 8.45s, respectively.

Based on the results illustrated in Figure 5, it seems that the radial RMS errors of the MLTOP method with the fitting time interval length of 18 hours are very low and far less than those of other configurations in Test 1 and Test 2. From Figure 6, it is indicated that the radial RMS errors of the MLTOP method with the fitting time interval length of 36 hours and 42 hours are very close in Test 1 and Test 2, and they are the lowest values among the results of all the configurations.

Through the comparative analysis of the above experiment results from Tables 1–4, it can be seen that, for the

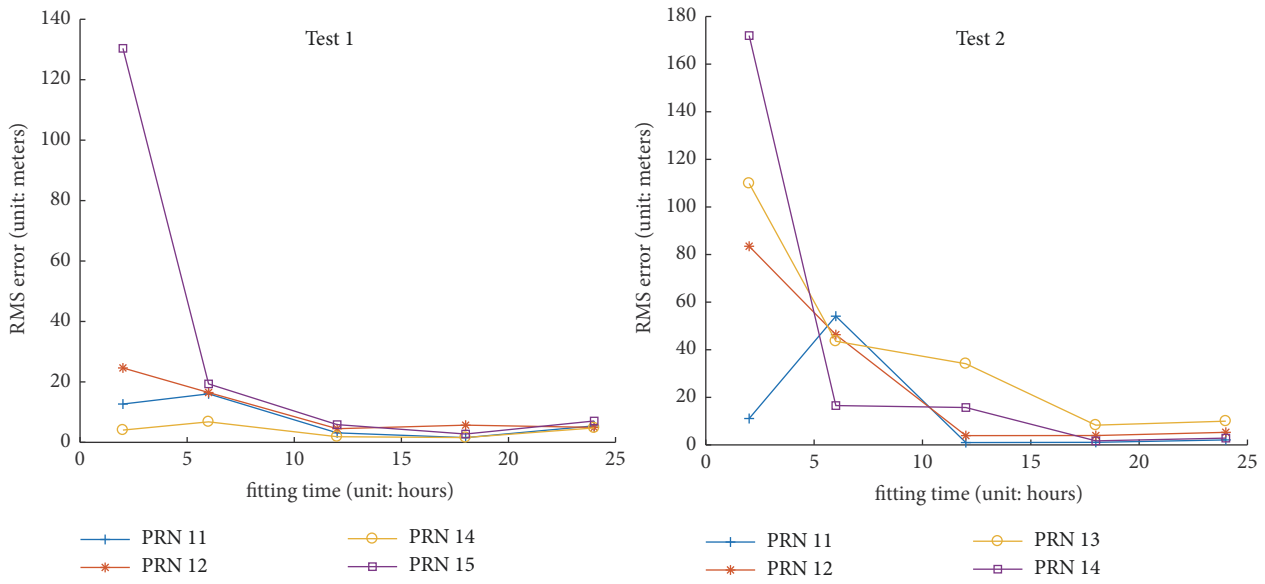

Figure 5: The radial RMS errors of the MLTOP method for the BeiDou MEO satellites with different fitting time intervals in Test 1 and Test 2.

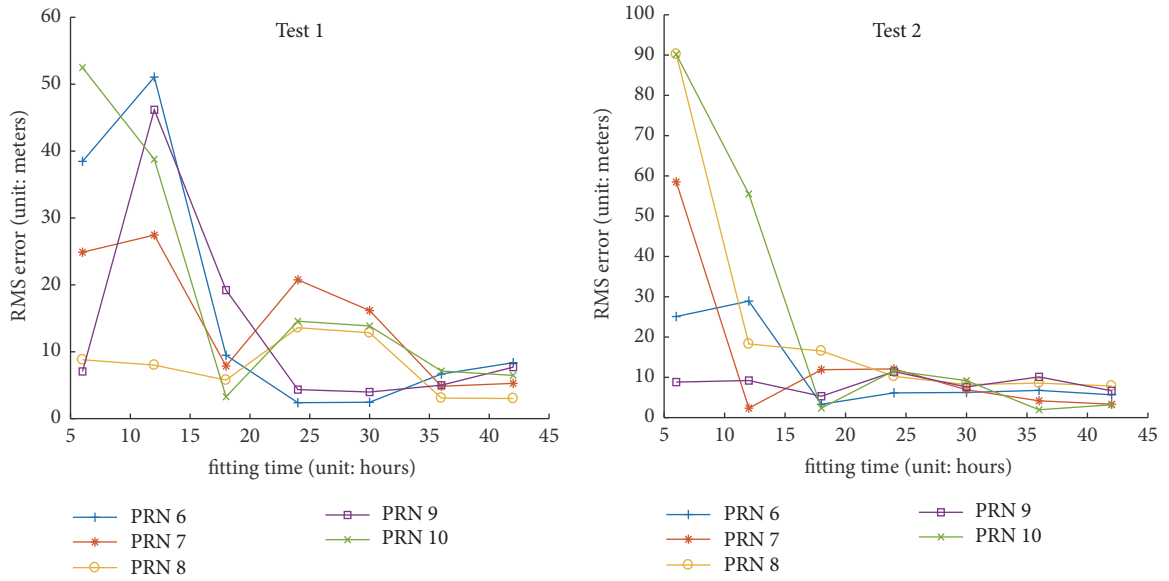

Figure 6: The radial RMS errors of the MLTOP method for the BeiDou IGSO satellites with different fitting time intervals in Test 1 and Test 2.

BeiDou satellites of different orbit types, the optimal fitting time interval length of the dynamic MLTOP method, in terms of result accuracy and time-consumption, is also different. In the case of BeiDou MEO satellites, the optimal fitting time interval length is about 18 hours, while the optimal fitting time interval length is about 36 hours in the case of BeiDou IGSO satellites. The optimal fitting time interval length for the IGSO satellites is much longer than that of the MEO satellites. One possible reason is that the orbital periods of these two types of satellites are different. For the BeiDou MEO satellites, the orbital period is about 12.89 hours, and for the BeiDou IGSO satellites, the orbital period is about 24 hours [19].

The update time of the BDS satellites' broadcast ephemeris data is one hour [33]. For the BeiDou MEO and IGSO satellites, the optimal time period needed to generate the predicted ephemeris is 18 hours and 36 hours, respectively. Thus, the number of required broadcast ephemeris sets is 18 and 36, respectively. For A-BDS receiver, when there is a communication connection, the historical broadcast ephemeris data can be shared with each other via the communication network, or supplementary broadcast ephemeris data can be obtained from the assistance data servers. When the A-BDS receiver is powered on for real-time positioning, the received broadcast ephemeris data can

Table 1: 3D error statistics of the MLTOP method for the BeiDou MEO satellites with different fitting time intervals (unit: meters).

Fitting time		PRN codes				
		11	12	13	14	15
Test 1	2 hours	58.78	99.35	--	24.95	287.06
	6 hours	65.65	83.04	--	33.68	106.85
	12 hours	20.57	21.54	--	10.81	64.70
	18 hours	17.01	18.61	--	7.94	18.86
	24 hours	34.31	19.50	--	26.34	24.20
Test 2	2 hours	273.04	497.95	278.16	389.04	--
	6 hours	262.74	253.24	173.57	126.89	--
	12 hours	23.80	29.10	141.13	88.05	--
	18 hours	30.26	31.98	44.94	26.02	--
	24 hours	28.47	32.01	54.69	24.95	--

Table 2: Radial error statistics of the MLTOP method for the BeiDou MEO satellites with different fitting time intervals (unit: meters).

Fitting time		PRN codes				
		11	12	13	14	15
Test 1	2 hours	12.69	24.64	--	4.08	130.40
	6 hours	16.06	16.50	--	6.80	19.34
	12 hours	3.15	4.54	--	1.87	5.89
	18 hours	1.58	5.70	--	1.60	2.77
	24 hours	5.48	4.95	--	4.77	7.08
Test 2	2 hours	11.09	83.5	109.90	172	--
	6 hours	54.10	46.33	43.58	16.54	--
	12 hours	0.99	3.93	34.11	15.71	--
	18 hours	1.11	3.94	8.30	1.73	--
	24 hours	2.13	5.31	10	2.87	--

be stored in the receiver's memory, and historical broadcast ephemeris data can be maintained by the background service program in the A-BDS receiver. In this way, new broadcast ephemeris data can be updated in real time.

If the historical broadcast ephemeris' outdate time is too long, the positioning accuracy will be degraded. Besides that, it will also have an important impact on the A-BDS receiver's uncertainty in the position domain during the navigation signal acquisition process [5]. However, at this time, it is still possible to use the long-term extended ephemeris for the First Fix. It is also feasible to perform a one-week satellite orbit prediction based on the outdated broadcast ephemeris data, but it will cause a certain degree of degradation of the predicted orbit accuracy.

In order to evaluate the predicted satellite clock bias errors, the 1-order and 2-order polynomial models are used to fit and predict the BeiDou MEO/IGSO satellite clock bias; then results are compared with the precise satellite clock bias data. The RMS error of predicted BeiDou IGSO satellite clock bias is shown in Table 5. The RMS error of predicted BeiDou MEO satellite clock bias is shown in Table 6. It should be noted that, according to the data obtained from the project IGS-MGEX and IGMAS, the ephemeris data of PRN 13 BeiDou satellite was missing in Test 1, and the ephemeris data of PRN 15 BeiDou satellite was missing in Test 2.

From Tables 5 and 6, it can be seen that, for the PRN 06, 07, 08, 10, and 11 BeiDou satellites, the 1-order polynomial model can be used to obtain the optimal prediction results. For the PRN 09, 12, 13, 14, and 15 BeiDou satellites, the 2-order polynomial model can be used to obtain the optimal prediction results. For all the BeiDou MEO/IGSO satellites, the mean RMS error of the predicted satellite clock bias is about 20 meters. This result is particularly similar to the JPL's predicted clock states. During the one-week prediction period, the largest contribution of the JPL's predicted clock to the URE index is about 28 meters [15]. Compared with the error of the predicted orbit, the error of predicted clock has a greater impact on the URE index. The test results also show that, in order to get more accurate prediction results of the satellite clock bias, it is an effective solution to select the polynomial model for satellite clock prediction with different order according to the statistical characteristics of the BeiDou satellite clock.

3.2. The Simulation Tests of SAFF Method with Ephemeris Extension. Based on the characteristics of the medium- and long-term extended ephemeris, we designed a set of simulation experiments, of which the plane sinusoidal trajectory of a ground vehicle was simulated, and the ground vehicle was equipped with a A-BDS receiver, which had the extended ephemeris stored in the memory. The date of simulation was

Table 3: 3D error statistics of the MLTOP method for the BeiDou IGSO satellites with different fitting time intervals (unit: meters).

Fitting time		PRN codes				
		06	07	08	09	10
Test 1	6 hours	173.85	98.77	66.99	42.80	202.85
	12 hours	232.45	96.34	37.42	213.90	117.69
	18 hours	71.09	28.84	48.53	88.08	20.62
	24 hours	53.44	49.30	56.64	33.42	44.35
	30 hours	57.15	41.94	55.22	33.77	47.75
	36 hours	50.80	43.00	29.63	34.62	52.59
	42 hours	49.73	42.38	33.29	33.67	54.90
Test 2	6 hours	311.42	247.31	494.27	114.40	402.61
	12 hours	306.70	43.82	106.51	174.33	279.78
	18 hours	97.13	40.58	65.32	115.55	55.59
	24 hours	63.88	35.73	63.94	83.78	35.32
	30 hours	66.08	28.10	60.62	93.10	33.37
	36 hours	56.41	29.73	62.60	90.31	24.72
	42 hours	56.71	31.05	65.56	84.42	30.08

Table 4: Radial error statistics of the MLTOP method for the BeiDou IGSO satellites with different fitting time intervals (unit: meters).

Fitting time		PRN codes				
		06	07	08	09	10
Test 1	6 hours	38.47	24.88	8.81	7.06	52.49
	12 hours	51.06	27.45	8.01	46.17	38.77
	18 hours	9.48	7.87	5.77	19.23	3.27
	24 hours	2.39	20.76	13.60	4.35	14.57
	30 hours	2.45	16.16	12.84	3.98	13.86
	36 hours	6.67	4.85	3.08	5.00	7.12
	42 hours	8.37	5.28	3.01	7.70	6.47
Test 2	6 hours	25.1	58.52	90.23	8.84	90.19
	12 hours	28.92	2.37	18.29	9.22	55.53
	18 hours	3.32	11.91	16.55	5.32	2.37
	24 hours	6.15	12.10	10.26	11.42	11.65
	30 hours	6.25	6.92	8.20	7.61	9.19
	36 hours	6.77	4.19	8.58	10.12	1.95
	42 hours	5.67	3.33	7.86	6.67	3.20

Table 5: RMS error statistics of the predicted BeiDou IGSO satellite clock bias with different model orders (unit: meters).

Model order		PRN codes				
		06	07	08	09	10
Test 1	1	25.54	18.45	17.55	38.95	9.22
	2	129.17	66.56	35.84	15.17	134.64
Test 2	1	25.34	24.80	21.59	21.24	19.17
	2	120.99	102.5	111.78	18.75	66.48

Table 6: RMS error statistics of the predicted BeiDou MEO satellite clock bias with different model orders (unit: meters).

Model order		PRN codes				
		11	12	13	14	15
Test 1	1	16.64	24.22	--	111.64	68.71
	2	128.0	19.84	--	14.84	9.19
Test 2	1	18.59	14.10	24.76	42.69	--
	2	27.58	13.93	6.03	14.47	--

set to 2016-10-13. We used the high-precision observation simulation algorithm to generate the observation data for all the visible BeiDou satellites. In the simulation software, the satellite orbit data and clock data were obtained from the real precise ephemeris file of that day, while the broadcast ephemeris data of that day, simulated with extended ephemeris errors, were used to estimate the position of the receiver.

In order to evaluate the influence of EE on the accuracy of the SAFF method, the medium- and long-term extended ephemeris error, according to the results error statistics of the

Table 7: The results error of the SAFF method using the BeiDou GEO satellites with real-time broadcast ephemeris and MEO/IGSO satellites with medium- and long-term EE.

Error type	X (m)	Y (m)	Z (m)	CEP (m)	SEP (m)
Results error	12.02	19.92	16.42	11.94	25.0

previous experiments, was added to the simulated observation. For the simulated observation of BeiDou MEO/IGSO satellite, the ephemeris error was simulated as the random variable with normal distribution, of which the mean was 0 and the variance was the RMS statistics of the extended ephemeris error. For the BeiDou MEO/IGSO satellites, the variance in the radial direction of the ECEF coordinate system was set to 8 m. To simulate the satellite clock bias error of BeiDou MEO/IGSO satellites, the clock bias error with the variance of about 20 meters was added to the simulated observation.

When the observation simulation was finished, the real broadcast ephemeris and the simulated observation data were used in the position estimation with the Weighted Least Squares (WLS) method. The corresponding results can be used to evaluate the accuracy of the SAFF method with medium- and long-term EE, where the evaluation index was the CEP and SEP. The CEP value can be used to evaluate the positioning accuracy in the horizontal direction. The SEP value can be used to evaluate the overall positioning accuracy.

This SAFF method requires the receiver to accomplish the frame synchronization and the complete broadcast ephemeris decoding of the BeiDou GEO satellites. The evaluation index of this SAFF method's results is shown in Table 7. In the calculation of the simulated observations, the medium- and long-term extended ephemeris error was not added to the observation of the GEO satellites. However, the extended ephemeris error was added to the observation of the MEO/IGSO satellites.

For the SAFF method using the BeiDou GEO satellites with real-time broadcast ephemeris and MEO/IGSO satellites with medium- and long-term EE, in this simulation experiment, the RMS error statistics in the X, Y, and Z directions of the ECEF coordinate system are 12.02 m, 19.92 m, and 16.42 m, respectively. The positioning accuracy in the horizontal direction is about 12 meters, while the overall positioning accuracy is about 25 meters. In [10], the mean of the horizontal position RMS after 7 days, with EE of GPS satellites, is about 12.35 m; this result is close to that of the simulation experiment in this paper, which also verifies the correctness of this SAFF method.

4. Conclusions

In this paper, we analyze the application model of the medium- and long-term extended ephemeris to assist the First Fix of the BDS receivers and put forward the SAFF method with the medium- and long-term EE. By using the actual ephemeris data, the accuracy of the medium- and long-term extended ephemeris is evaluated. Through the simulation experiments, the accuracy of the SAFF method with medium- and long-term EE is assessed. The highlights of this work are as follows.

(1) In the SAFF method of the BDS receivers, the medium- and long-term extended ephemeris of the BeiDou MEO/IGSO satellites can be used instead of the real-time broadcast ephemeris. However, for the BeiDou GEO satellites, the accuracy of the medium- and long-term extended ephemeris is too low to be used in the SAFF method.

(2) In the SAFF method of the BDS receivers, all the visible BeiDou satellites are used, where the medium- and long-term extended ephemeris is used for the MEO/IGSO satellites, and the real-time broadcast ephemeris is used for the GEO satellites. For this SAFF method with the medium- and long-term extended ephemeris, the horizontal positioning accuracy is about 12 meters and the overall positioning accuracy is about 25 meters. The corresponding TTFF is about 8~14 seconds, and the reduced time of the TTFF is at least 20s when compared with that of the conventional BDS receivers.

(3) In order to obtain the optimal positioning accuracy and time-consumption of the MLTOP method for the BeiDou MEO satellites, the 10∗10-order EGM-96 earth gravity field model is adopted in the case of orbit fitting time interval configured as about 18 hours long. For the BeiDou IGSO satellites, the orbit fitting time interval is configured as about 36 hours, and the MLTOP results with the best performance in terms of accuracy and time-consumption can be obtained.

There are also some limitations in this SAFF method with medium- and long-term EE. For instance, to get the results with enough accuracy, the fitting time interval length of the dynamic MLTOP method for the BeiDou IGSO satellites is quite long, about 36 hours, which needs more ephemeris data. Therefore, this method requires the BDS receivers to receive and store the broadcast ephemeris over a span of long enough time interval, which limits the application of this method in the mobile device. In addition, the prototype program, limited to the existing experimental environment, was just implemented on a PC platform, so the time-consumption results just reflected the relative speed between different configurations of the dynamic MLTOP method. However, the results may then serve as guidelines for future work. To evaluate time-consumption results in the actual scene, first extension of our work may be porting the prototype program to the embedded platform of the BDS receivers.

In order to adapt to different communication connection conditions, for the future research on the self-assisted A-BDS receiver, we will consider how to optimize the method of obtaining the EOP parameters in an integrated manner. For example, adaptively selecting between the joint estimation method of the EOP parameters and the EOP

data transmission method through the network connection. According to the current communication connection conditions of the A-BDS receiver, the comprehensive combination of the autonomous and nonautonomous generated EE will greatly improve the reliability and flexibility of the First Fix of the A-BDS receiver. In addition, with the development of A-GNSS technology, a multiconstellation solution will provide more options for solving the problem related to the SAFF method.

Abbreviations

GNSS:	Global Navigation Satellite System
BDS:	BeiDou Navigation Satellite System
GPS:	Global Positioning System
PNT:	Positioning, Navigation, and Timing
UAV:	Unmanned Aerial Vehicles
LBS:	Location-Based Services
TTFF:	Time to First Fix
EE:	Ephemeris Extension
MLTOP:	Medium- and Long-Term Orbit Prediction
SAFF:	Self-Assisted First Fix
MLTO:	Medium- and Long-Term Orbit
EGM-96:	Earth Gravitational Model 1996
EGM-08:	Earth Gravitational Model 2008
JGM-3:	Joint Gravity Model 3
RKF:	Runge-Kutta-Fehlberg
3D:	3-Dimensional
URE:	User Range Error
ECEF:	Earth Centered Earth Fixed
ECI:	Earth Centered Inertial
LS:	Least Squares
IGS:	International GNSS Service
IGS-MGEX:	International GNSS Service Multi-GNSS Experiment
IGMAS:	International GNSS Monitoring & Assessment System
ICD:	Interface Control Document
LEO:	Low Earth Orbit
AR:	Autoregression
SRP:	Solar Radiation Pressure
PRN:	Pseudo Random Noise
SP3:	Standard Product #3
RAC:	Radial, along-track, cross-track
ARMA:	Autoregressive and Moving Average
MEO:	Medium Earth Orbit
IGSO:	Inclined Geosynchronous Satellite Orbit
GEO:	Geostationary Earth Orbit
RMS:	Root Mean Square
A-BDS:	Assisted BDS
CEP:	Circular Error Probable
SEP:	Spherical Error Probable
EOP:	Earth Orientation Parameter
IERS:	International Earth Rotation and Reference Systems Service
4G:	The 4th-Generation mobile communication technology
5G:	The 5th-Generation mobile communication technology.

Data Availability

The data used to support the findings of this study are available from the corresponding author upon request.

Disclosure

The affiliation "College of Space Information, Space Engineering University" is the new name of the university, whose original name was the Department of Information Equipment in the Academy of Equipment Command and Technology.

Conflicts of Interest

The authors declare that there are no conflicts of interest.

Acknowledgments

The work described in this paper is supported by the National Natural Science Foundation of China (no. 41604016). The authors acknowledge the IGS, the IGS CDDIS analysis center, the IGS-MGEX project, and the IGMAS project for providing the valuable data and products.

References

[1] E. G. N. S. S. Agency. GNSS Market Report 2017.

[2] S. Fuping, S. Liu, X. Zhu, and B. Men, "Research and progress of Beidou satellite navigation system," *Science China Information Sciences*, vol. 55, no. 12, pp. 2899–2907, 2012.

[3] X. Li, M. Ge, X. Dai et al., "Accuracy and reliability of multi-GNSS real-time precise positioning: GPS, GLONASS, BeiDou, and Galileo," *Journal of Geodesy*, vol. 89, no. 6, pp. 607–635, 2015.

[4] L. Serrano, D. Kim, R. B. Langley, K. Itani, and M. Ueno, "A GPS Velocity Sensor: How Accurate Can It Be? - A First Look," in *Proceedings of the ION NTM 2004*, vol. 2004, pp. 875–885, San Diego, CA, USA.

[5] F. v. Diggelen, *A-GPS: Assisted GPS, GNSS, and SBAS*, Artech House, Boston, Mass, USA, 2009.

[6] R. N. Inc. Product Brief Predicted GNSS Ephemeris.

[7] E. G. Agency. GNSS USER TECHNOLOGY REPORT (ISSUE 1). 2016.

[8] M. Seppänen, J. Ala-Luhtala, R. Piché, S. Martikainen, and S. Ali-Löytty, "Autonomous Prediction of GPS and GLONASS Satellite Orbits," *Navigation: Journal of the Institute of Navigation*, vol. 59, no. 2, pp. 119–134, 2012.

[9] M. Seppänen, T. Perälä, and R. Piché, "Autonomous satellite orbit prediction," in *Proceedings of the Institute of Navigation - International Technical Meeting 2011, ITM 2011*, pp. 554–564, January 2011.

[10] Y. Li and Y. Gao, "Navigation performance using long-term ephemeris extension for mobile device," in *Proceedings of the 26th International Technical Meeting of the Satellite Division of the Institute of Navigation, ION GNSS 2013*, pp. 1642–1651, September 2013.

[11] Y. Li, Z. Nie, S. Chen, and Y. Gao, "Multiple Constellation Navigation Performance Using Long-Term Ephemeris Extension with Backward Error Representation," in *Proceedings of the ION PNT 2015*, HonoLulu, HI, USA, 2015.

[12] M. M. Romay and M. D. Láinez, "Generation of precise long-term orbit and clock prediction products for A-GNSS," in *Proceedings of the 25th International Technical Meeting of the Satellite Division of the Institute of Navigation 2012, ION GNSS 2012*, pp. 3122–3139, September 2012.

[13] L. Garin, *Ephemeris Extension Method for GNSS applications*, USA Patent, 2009.

[14] http://rxnetworks.com/location-io/predicted–gnss-ephemeris/.

[15] http://www.gdgps.net/products/predicted-orbit.html.

[16] X. Gang, *Principles of GPS and Receiver Design*, Publishing House of Electronic Industry, Beijing, China, 1st edition, 2009.

[17] O. Montenbruck and E. Gill, *Satellite Orbits: Models, Methods and Applications*, Springer, Berlin, Germany, 2000.

[18] Q. Zhao, *Research on Precise Orbit Determination Theory and Software of GPS Constellation and LEO Satellite*, Wuhan, China, Wuhan University, 2004.

[19] J. Tang, X. Hou, and L. Liu, "Long-term evolution of the inclined geosynchronous orbit in Beidou Navigation Satellite System," *Advances in Space Research*, vol. 59, no. 3, pp. 762–774, 2017.

[20] J. Chen and J. Wang, "Reduced-Dynamic Precise Orbit Determination for Low Earth Orbiters Based on Helmert Transformation," *Acta Geodaetlca et Cartographica Sinica*, vol. 37, no. 3, pp. 394–399, 2008.

[21] http://www.igs.org/products.

[22] M. Seppänen, J. Ala-Luhtala, R. Piché, S. Martikainen, and S. Ali-Löytty, "Autonomous prediction of GPS and GLONASS satellite orbits," *NAVIGATION: Journal of the Institute of Navigation*, vol. 59, no. 2, pp. 119–134, 2012.

[23] L. Wenming, L. Zhengrong, L. Wenxiang, and W. Feixue, "Influence of EOP Prediction Errors on Orbit Prediction of Navigation Satellites," *GNSS World of China*, vol. 34, no. 6, pp. 17–22, 2009.

[24] https://www.iers.org/IERS/EN/DataProducts/EarthOrientationData/eop.html.

[25] A. Osseiran, J. F. Monserrat, Y. P. Marsch et al., *5G Mobile and Wireless Communications Technology*, Cambridge University Press, Cambridge, UK, 2016.

[26] F. Cao, X. Yang, Z. Li et al., "Orbit determination and prediction of GEO satellite of BeiDou during repositioning maneuver," *Advances in Space Research*, vol. 54, no. 9, pp. 1828–1837, 2014.

[27] S. Jing, W. Liu, L. Yong, and G. Sun, "A Quick A-BDS Location Method Based on Characteristics of GEO Satellite and Ridge Estimate," in *Proceedings of the China Satellite Navigation Conference (CSNC) 2015*, vol. 340, pp. 739–747, Nanjing, China, 2015.

[28] O. Montenbruck, P. Steigenberger, R. D. Khachikyan, U. Hugentobler et al., "IGS-MGEX: preparing the ground for multi-constellation GNSS science," *Inside GNSS*, vol. 9, no. 1, pp. 42–49, 2014.

[29] J. Wenhai, D. Qun, L. Jian-wen et al., "Monitering and Assessment of GNSS Open Services," *Journal of Navigation*, vol. 64, no. S1, pp. S19–S29, 2011.

[30] Global Positioning System Satndard Positioning Service Performance Standard, Department of Defense, USA, o. A. a. G. Navstar, Ed., 4th ed, 2008.

[31] U. DoD, *Global positioning system standard positioning service performance standard*, 2008.

[32] Z. Shifeng, Y. Huabo, and C. Hong, *Inertial Guidance Weapon Precision Analysis and Evaluation*, NUDT Press, Changsha, China, 2008.

[33] C. S. N. Office. BeiDou Navigation Satellite System Signal In Space Interface Control Document Open Service Signal B3I (Version 1.0). 2018.